Sumnall, Matthew J.; Hill, Ross A.; Hinsley, Shelley A**.** 2016. **Comparison of small-footprint discrete return and full waveform airborne lidar data for estimating multiple forest variables.**

*Revised Manuscript with no Changes Highlighted

Comparison of small-footprint discrete return and full waveform airborne lidar data for estimating multiple forest variables

Matthew J. Sumnall[a,b], Ross A. Hill[b], Shelley A. Hinsley[c]

[a] *Virginia Polytechnic Institute and State University, Department of Forest Resources and Environmental Conservation, Blacksburg, VA 24061, USA.*

[b] *Department of Life and Environmental Sciences, Bournemouth University, Poole, Dorset, UK.*

[c] *Centre for Ecology and Hydrology, Wallingford, Oxfordshire, UK.*

Abstract:

The quantification of forest ecosystems is important for a variety of purposes, including the assessment of wildlife habitat, nutrient cycles, timber yield and fire propagation. This research assesses the estimation of forest structure, composition and deadwood variables from small-footprint airborne lidar data, both discrete return (DR) and full waveform (FW), acquired under leaf-on and leaf-off conditions. The field site, in the New Forest, UK, includes managed plantation and ancient, semi-natural, coniferous and deciduous woodland. Point clouds were rendered from the FW data through Gaussian decomposition. An area-based regression approach (using Akaike Information Criterion analysis) was employed, separately for the DR and FW data, to model 23 field-measured forest variables. A combination of plot-level height, intensity/amplitude and echo-width variables (the latter for FW lidar only) generated from both leaf-on and leaf-off point cloud data were utilised, together with individual tree crown (ITC) metrics from rasterised leaf-on height data. Statistically significant predictive models ($p < 0.05$) were generated for all 23 forest metrics using both the DR and FW lidar datasets, with R^2 values for the best fit models in the range $R^2 = 0.43$ - 0.94 for the DR data and $R^2 = 0.28$ - 0.97 for the FW data (with normalised RMSE values being 18% - 66% and 16% - 48%

respectively). For all but two forest metrics the difference between the NRMSE of the best performing DR and FW models was ≤ 7%, and there was an even split (11:12) as to which lidar dataset (DR or FW) generated the best model per forest metric. Overall, the DR data performed better at modelling structure variables, whilst the FW data performed better at modelling composition and deadwood variables. Neither showed a clear advantage at modelling variables from a particular vegetation layer (canopy, shrub or ground). Height, intensity/amplitude, and ITC-derived crown variables were shown to be important inputs across the best performing models (DR or FW), but the additional echo-width variables available from FW point data were relatively unimportant. Of perhaps greater significance to the choice between lidar data type (i.e. DR or FW) in determining the predictive power of the best performing models was the selection of leaf-on and/or leaf-off data. Of the 23 best models, 10 contained both leaf-on and leaf-off lidar variables, whilst 11 contained only leaf-on and two only leaf-off data. We therefore conclude that although FW lidar has greater vertical profile information than DR lidar, the greater complimentary information about the entire forest canopy profile that is available from both leaf-on and leaf-off data is of more benefit to forest inventory, in general, than the selection between DR or FW lidar.

Keywords: remote sensing; forest inventory, airborne laser scanning; area-based regression

1. Introduction

A forest ecosystem can be described in terms of its structural, compositional and functional properties, which can be strongly influenced by any management strategies applied to a site. The quantification of forest structure is important for a range of disciplines, as vegetation structure is related to a wide variety of ecosystem processes. However, a comprehensive understanding of the overall spatial patterns of structural variation in large forested landscapes is still largely incomplete (Anderson et al., 2008).

The management of an area is often assisted by landscape-scale monitoring (Newton et al., 2009), with a requirement of measuring both vertical and horizontal metrics. For example, the assessment of timber yields requires information on the density of trees, together with their species and size (Matthews & Mackie, 2006). Such data allow the quantification of timber yield and its associated economic value, and in addition risk assessment for fire, wind or pest damage, which are also partially dependent on canopy structure. Vertical structure is of importance in determining the species composition of ground flora (Ferris et al., 2000), in the assessment of habitat quality for many forest-dwelling species (Hinsley et al., 2009), and as an indicator of biodiversity (Ferris & Humphrey, 1999). Traditionally forest inventory data are collected through manual field observations in sample plots. The benefit of this approach can be high accuracy, but it is time consuming and expensive (Aplin, 2005).

Airborne remote sensing technologies such as lidar can characterise both horizontal and vertical structures in forested environments. The use of lidar has rapidly come to prominence in estimating forest biophysical characteristics, such as canopy height and basal area (Evans et al, 2009). Most commercial airborne lidar systems are small-footprint (i.e. < 1m) and deliver discrete return (DR) point data. The point data correspond to high intensities in the back-scattered light of the laser pulse interacting with a surface, allowing some systems to record multiple returns per laser pulse (typically 1 - 5). Due to limitations in the design of most multi-return airborne lidar systems, there is a sizable 'blind spot' (or dead zone) following each detected return (typically 1.2 m to 5.0 m) in which no other surfaces can be detected (Reitberger et al., 2008). Range resolution is determined by the length of the transmitted pulse and the maximum number of returns recorded by the sensor. The signal processing algorithms which are used to detect returns are often proprietary and differ between DR lidar sensors (Disney et al., 2010; Næsset, 2009).

Recent developments in scanning lidar technology resolve the issue of a blind spot. Small-footprint, full waveform (FW) lidar systems have become available commercially. FW lidar sensors digitize the total amount of laser energy returned to the sensor in fixed time intervals (typically 1 ns to 5 ns), providing a near continuous distribution of back-scattered laser intensity for each recorded pulse (Wagner et al., 2008). Instead of clouds of individual three-dimensional points, such as with DR lidar, small-footprint FW lidar devices provide connected profiles of the three dimensional scene, which contain more detailed information about the structure of the illuminated surfaces (Alexander et al., 2010). Each waveform consists of a series of temporal modes (or echoes), where each corresponds to an individual reflection event from an object or set of close but separated objects. Each laser pulse waveform represents complex data, which requires sophisticated processing before metrics can be generated (Chauve et al., 2009). One potential approach to derive information from the waveform is to identify proximal peaks, or returns, to present the waveform as a series of Gaussian curves; fitted by a non-linear least squares approach (Miura & Jones, 2010; Wagner et al., 2006). The replacement of Gaussian functions with stochastic functions based on marked point processes (Mallet et al., 2010) has also been suggested as a method of processing small-footprint FW lidar data. Extracting individual returns from FW data can have the effect of removing the blind spot present in DR data that have been processed by proprietary software.

Airborne DR lidar systems have been utilised for the estimation and retrieval of various forest related variables, which are important to management and ecological monitoring. This is due to an inherent ability to provide both geo-referenced horizontal and vertical information on the structure of forest canopies, with sampling dependent on the type of lidar system used and flight configuration (Evans et al., 2009; Næsset, 2009). The most obvious vegetation measure extracted from lidar is that of canopy height. Plot- or stand-level regression analysis or non-parametric model estimates of canopy density, mean tree height, basal area and volume have been applied (Bouvier et al. 2015; Hyyppä et al., 2008; Næsset, 2007). Other studies have been able to characterise understorey vegetation cover and detect suppressed trees (Estornell et al., 2011; Maltamo et al., 2005), assess regeneration patterns and floristic composition (Bollandsås et al., 2008; Leutner et al., 2012), and estimate deadwood volume (Kim et al., 2009b; Pesonen et al., 2008). Lidar sensors, typically DR, can collect data at point densities sufficient to identify individual tree crowns in forest canopies and delineate crown horizontal extent and vertical depth (Kaartinen et al., 2012). Such individual tree crown (ITC) metrics have been identified as important inputs into predicative models of forest variables (e.g. Hyyppä et al., 2001; Persson et al., 2002; Popescu et al., 2004).

With an increasing accessibility of small-footprint FW lidar, there is a small but growing number of published studies which evaluate FW and DR lidar for the estimation of forest structural and compositional parameters. For example, Cao et al. (2014) compared statistical predictions of total living biomass obtained from DR lidar metrics (i.e. height and height variance measures, canopy return density measures, and canopy cover measures) and from FW lidar metrics (i.e. height of median energy, waveform distance, height/median ratio, number of peaks, roughness of outermost canopy, front slope angle, return waveform energy and vertical distribution ratio). They extracted the DR data by Gaussian decomposition of the FW data, and therefore the two datasets shared the same sampling rate characteristics but supplied different sets of metrics due to the way the full waveform information was processed. They found that lidar metrics related to canopy height (either DR or FW derived) were the strongest predictors of total biomass, but that there were benefits from the synergistic use of DR and FW lidar metrics in estimating the different biomass pools in the forest vertical structure. Lindberg et al. (2012) outlined a method to analyse both DR and FW lidar data for the estimation of canopy vegetation volume for coniferous and deciduous forest. Estimates of volume from FW lidar were predicted more accurately than from DR lidar, especially when corrections were applied for the shielding effects of higher vegetation layers based on the Beer-Lambert Law. Allouis et al. (2013) reported similar results where the inclusion of FW metrics improved model estimates for the prediction of above-ground biomass of individual trees, but gave slightly inferior estimates of stem volume when compared with DR lidar only. Yu et al. (2014) compared DR and FW lidar for individual tree crown delineation and boreal forest species classification, reporting that FW lidar was slightly better for detecting trees, whilst DR metrics combined with FW metrics improved species classifications. Armston et al. (2013) compared DR and FW lidar data for the estimation of vertical canopy gap probability for savanna woodland, showing that models produced using FW lidar data were superior.

The use of small-footprint DR lidar data for forest inventory using an area-based regression approach is now well established (Næsset, 2007). As small-footprint FW lidar data become more readily available, early studies suggest possible benefits and potential drawbacks in moving towards these data. As yet there has been no systematic study to compare small-footprint DR and FW data for the estimation of multiple inventory variables from across a forest profile. This study addresses this research gap, comparing point cloud data and derived products from DR lidar and from Gaussian decomposition of FW lidar. The work of Cao et al. (2014) compared standard DR height metrics with newer sets of FW lidar metrics, and specifically avoided investigating the effects of higher density point clouds provided by FW lidar decomposition. Here we specifically focus on a comparison between the different information content on forest vertical and horizontal structure and recorded return pulse characteristics in DR and FW-derived point clouds. We assess 23 common forest inventory variables covering all forest vegetation layers (canopy, shrub and ground layer) and both living and dead wood. Airborne DR and FW lidar data were acquired simultaneously under both leaf-on and leaf-off conditions, and variables from both (including point cloud and ITC-derived lidar variables) are used in area-based regression modelling of forest inventory variables. The wider context of this work was forest condition assessment.

2. Data and Methods

2.1 Study site

The study site is located within the New Forest National Park, between Southampton and Bournemouth, in southern England (lat: 50° 50' N, long: 1° 30' W). This National Park has multiple land covers and land uses, with much of the forested area actively managed (see Tubbs 2001). This study is focused on a ca. 22 km^2 area that sits in a triangle between the villages of Lyndhurst, Brockenhurst, and Beaulieu. This area is low lying, between 5m and 45m above sea level, with only gently undulating terrain. The forest includes managed inclosures, in addition to unenclosed areas which are not subject to felling operations and are permanently open to grazing by large ungulates (mostly ponies, deer and cattle).

The study area contains several types of semi-natural and plantation coniferous and deciduous forests in close proximity (Newton et al., 2010). Deciduous species include: oaks (*Quercus robur* and *Quercus petrea*), beech (*Fagus sylvatica*), common alder (*Alnus glutinosa*), silver birch (*Betula pendula*), sweet chestnut (*Castanea sativa*), and holly (*Ilex aquifolium*). Coniferous species include: Corsican pine (*Pinus nigra* var. maritime), Scots pine (*Pinus sylvestris*), Douglas fir (*Pseudotsuga menziesii*) and Norway spruce (*Picea abies*). This array of forest types within close proximity to each other presents a wide range of available structural and compositional variables of interest, such as canopy gaps and the presence of deadwood or understorey.

2.2 Field data collection

Using pre-existing data, the woodland areas of the study site were split into coniferous, deciduous and mixed woodland compartments and stratified according to their relative biomass, as derived from Normalised Difference Vegetation Index (NDVI) data. A total of 41 field plots were then randomly located across this stratification to enumerate a range of forest types and canopy conditions. An initial 21 plots were visited in the summer of 2010 (subsequently used for establishing relationships), with the remaining 20 plots visited in a further field campaign in the summer of 2012 (used for validating relationships). The field plots were only enumerated if they were located a minimum of 10 m away from a stand boundary in order to limit any potential edge effects.

Field data were collected from north-oriented 30 m × 30 m plots with a 10 m × 10 m subplot in the south-west corner. Plot positions were located accurately using a combination of a Leica GPS 500 (Leica Geosystems) and Sokkia 6F total station (SOKKIA TOPCON Co. Ltd.). Post-processing of the coordinates was performed in Leica Geo-office software (version 8.2). Total horizontal positional error was calculated as ≤ 0.08 m.

Plot-level totals and averages were calculated for each field recorded metric. Within each plot, diameter at breast height (DBH) was recorded at 1.3 m above the ground for every stem, and for those with DBH > 10 cm, a 3D position (via total station) was recorded to estimate stem spacing. In addition, canopy top height (m), height to the living crown (HTLC) (m), crown horizontal dimensions in the east-west and north-south directions, and species type were recorded. Vertical height measurements were calculated via trigonometry, using a measured horizontal distance from the tree stem and an angular measurement, from a clinometer, to the required vertical feature. Plot-level basal area was calculated by summing the area of a circle calculation applied to each tree DBH measurement within the plot extent. The number of stems of native tree species was recorded. Native tree species within the study site were considered to include Scots pine, common alder, oak, beech, silver birch, holly and sweet chestnut.

The species compositional indices of the Shannon-Wiener index (SH) (Shannon, 1948) and the Simpson index (SI) (Simpson, 1949) were utilised in this study. The Shannon-Wiener diversity index for all tree species was calculated as:

$$SH = \sum_{i=1}^{n} p_i \, log_e \, p_i \qquad [1]$$

where p_i = the proportion of individuals (plot stem number) in the *i*th species, and *n* is the number of species. The Simpson index was calculated for tree species in each plot as:

$$SI = 1 - \left(\sum_{i=1}^{n} (1 - p_i) p_i \right) \qquad [2]$$

where p_i = the proportion of individuals (plot stem number) in the *i*th species, and *n* is the number of species.

Each of the standing deadwood items, or snags, within a field plot was recorded. Snags were defined as standing deadwood > 10 cm DBH (Spies et al., 1988). Snag volume was calculated using the formula for determining cylindrical volume using height and girth measurements. Downed deadwood (DDW) was defined as deadwood logs or branches of at least 10 cm diameter lying on the ground (Spies et al., 1988). Measurements for DDW were made in the

10 m × 10 m sub-plot only. Length and girth around the maximum and minimum diameters of the log were recorded. Estimates of DDW volume were determined using the equation for a frustum of a cone. To assess deadwood decay class, snags and DDW were divided into three decay classes according to the following criteria, as defined in Cantarello & Newton (2008): (i) logs with a low decay state, no surface breakdown, bark still intact, wood structure firm; (ii) logs with a moderate decay state, with some surface breakdown, wood structure weaker but bole mostly sound; and (iii) logs with high decay state, extensive surface breakdown, bark mostly absent, bole with no sound wood present and colonised with vegetation. A size-weighted average decay class score was then calculated at the plot level.

The number of saplings and their species types (including the number of saplings of a native species) were recorded within each field plot. Saplings were defined as tree stems > 1.3 m in height with DBH < 10 cm. The total number of seedlings, their species type, and number of seedling stems of native species within the sub-plot extent were also recorded. Seedlings were defined as tree stems < 1.3 m in height. The number of vascular plant species and the percentage of bare ground within each 30 m × 30 m plot were also recorded.

In total, 23 forest variables were recorded in the field and subsequently investigated using airborne lidar data. Summary information of field data across the 21 plots surveyed in 2010 and 20 plots surveyed in 2012 is given in Table 1.

[insert Table 1 here]

2.3 Airborne lidar data collection

Small-footprint lidar data were acquired for the study area under leaf-off (April 8) and leaf-on (July 6) conditions in 2010. The lidar instrument used was the Leica ALS50-II airborne laser scanner with an upgrade to allow the simultaneous recording of DR and FW data. On both dates the lidar data were acquired at a flying altitude of ca. 1600 m, with a pulse repetition frequency (PRF) of 147 kHz, a beam divergence of 0.22 mr, and a scan half angle of 10^o. The geometric accuracy for the scanner is stated by the manufacturer (Leica Geosytems) as a nominal vertical accuracy of 0.05 m to 0.10 m, and horizontal accuracy of 0.13 m to 0.61 m. With the chosen flight and sensor configuration, the average sampling rate for the leaf-on and leaf-off data was 5.0 and 5.2 pulses m^{-2} respectively (including areas of flight-line overlap). The DR and FW data were recorded from the same set of emitted pulses, but the ALS50-II scanner could only digitise the full waveform of every other pulse at the PRF used for these acquisitions. In actuality, the sampling rate for the FW lidar data was slightly less than half that of the DR data quoted above (49% and 48% for the leaf-on and leaf-off data respectively) due to minor recording errors. The DR data had up to four discrete returns per laser pulse, with x-, y- and z-coordinates, intensity, and return number supplied for the first, intermediate, and last significant returns per pulse. For the FW data, 256 return signal amplitude values (sampled every two nanoseconds for the April data and every one nanosecond for the July data) were supplied for each laser pulse.

2.4 Airborne lidar data processing

The DR lidar data were supplied as LAS 1.0 format files, with a basic classification identifying noise returns already applied using Terrascan software (http://www.terrasolid.fi). A number of pre-processing steps were required before metrics could be derived from the lidar data for subsequent analysis. All of these steps were performed using the RSC LAS Tools software (version 1.9.3) (http://code.google.com/p/rsclastools). The DR point cloud data required filtering to separate the ground and vegetation hits so that ground elevation could be determined and used to normalise vegetation hits to above-ground height. RSC LAS Tools software employs a progressive morphological filter, as outlined in Zhang et al. (2003), to filter out ground returns, which were then interpolated into a surface at 1m resolution using the nearest neighbour method. Ground elevation values were then removed from the DR lidar dataset to yield vegetation height. All points which intersected within field plot locations were clipped from the dataset and used to create plot-level lidar variables, as in Falkowski et al. (2009) and Hudak et al. (2008). These included eight variables (mean, median, maximum, standard deviation, variance, absolute deviation, skewness and kurtosis) which were calculated from the height data (separately for all and non-ground returns) and from the intensity data (separately for all, non-ground and ground returns) for both leaf-on and leaf-off lidar acquisitions. This totalled 80 variables. In addition, percentiles at 5% intervals between 5% and 95% were created for both height and intensity data using all returns, separately for both leaf-on and leaf-off acquisitions. This totalled an additional 72 variables (as the maximum and median values were already calculated above).

In addition, canopy cover was calculated as:

$$CC = \left(\frac{h_{ng}}{h_{all}}\right) \quad [3]$$

where h_{ng} and h_{all} denote the sum total of non-ground returns and the sum of all returns, respectively. A vertical profile was generated by stratifying the frequency of all returns at the plot-level vertically for every metre. The number of vertical layers was estimated by iteratively fitting Weibull functions to the vertical profile (fit to the frequency of return height bins), where local maxima or ‘peaks’ were taken to represent vertical layers and troughs were taken to be layer divisions (Coops et al., 2007). The number of local maxima was considered to identify the number of vertical layers. The largest vertical separation between layers, or between a layer and ground, was then calculated for each plot to derive the largest vertical gap within the canopy profile. These three metrics (canopy cover, number of canopy layers, and the size of largest vertical canopy gap) were calculated separately for the leaf-on and leaf-off DR lidar data. Thus, a total of 158 metrics were derived from the DR point cloud data for each 30 m x 30 m field plot area.

The FW lidar data were provided in LAS 1.3 file format, containing GPS, IMU, and laser pulse return waveform data. The FW lidar pre-processing tasks were performed using the Sorted Pulse Software Library (SPDlib) (version 1.0.0) (Bunting et al., 2013a, 2013b). In order to derive 3D point information from the recorded waveforms, it was necessary to apply a process of Gaussian decomposition to each (as described in Wagner et al., 2006), identifying peaks in the return signal above a background threshold level representing noise. A combination of angular measurements, bearing, positional information of the aircraft and first peak coordinates, trigonometry and the relevant pulse timings (2 ns or 1 ns) allowed the estimation of the 3D locations for each of the fitted Gaussian peaks, in addition to peak attributes such as amplitude and width. This yielded between 1 and 11 returns per pulse, supplying x-, y- and z- coordinates, amplitude and width per return. The majority of pulses generated at least two returns in the leaf-on data and at least three returns in the leaf-off data, which compared with the majority of pulses generating only single returns in both the leaf-on and leaf-off DR lidar data. The sampling rates of the DR and FW point clouds are summarised in Table 2. Overall, the FW lidar provided more returns for each pulse than the DR lidar (and more information per return), supplying a higher vertical sampling rate (Figure 1). However, the total sampling rate was lower in the FW data, and in particular the horizontal sampling rate at the canopy surface was considerably higher in the DR data. This contrast in sample distribution between DR and FW lidar across the 3D volume of a forest landscape is the focus of the data comparison being made here.

[insert Table 2 & Fig 1 here]

The SPDlib software also provided tools for noise filtering, vegetation classification and height normalisation on the extracted point data. As with the DR data processing, this used the progressive morphological filter, as outlined in Zhang et al. (2003), to identify ground returns. The above-ground heights were then calculated by subtracting the ground elevation surface (as interpolated by a natural neighbour algorithm from the classified ground returns) from all returns. Subsequently, all returns which intersected within field plot locations were clipped from the dataset, and eight variables (mean, median, maximum, standard deviation, variance, absolute deviation, skewness and kurtosis) were calculated from the height data (separately for all and non-ground returns) and from both the amplitude and echo-width data (separately for all, non-ground and ground returns), all for both leaf-on and leaf-off lidar acquisitions. This totalled 128 variables. In addition, percentiles at 5% intervals between 5% and 95% were created for height, amplitude and echo-width data using all returns, separately for leaf-on and leaf-off acquisitions. This totalled an additional 108 variables. The metrics derived from analysis of the canopy horizontal and vertical profile (i.e. canopy cover, largest vertical gap, and number of vertical layers) were also calculated from leaf-on and leaf-off FW data in the same way as for the DR metrics. A total of 242 metrics were derived from the FW-derived point cloud data for each 30 x 30 m field plot area.

Individual tree crown (ITC) delineation techniques were implemented on the DR and FW lidar data (leaf-on only) using the Toolbox for Lidar Data Filtering and Forest Studies (TIFFS) software (version 5.0) (http://www.globalidar.com). A 1 × 1 m resolution raster Canopy Height Model (CHM) was created using the maximum above-ground height in each cell. Tree crowns were isolated using a marker-controlled watershed segmentation method, as used in Chen et al. (2006), where tree top positions were located and regions 'grown' into areas of decreasing height. The identification of individual tree crowns was performed separately using leaf-on DR and FW lidar data, resulting in a GIS database of individual tree locations and crown attributes. Note that ITC objects with a crown horizontal radius < 1.5 m or a height ≤ 1.3 m were removed from this database as non-tree features. All remaining ITC objects with a centroid within the field plot extent were extracted and this was used to generate eight plot-level ITC variables for both the DR and FW data: mean tree height, mean and total crown area, mean and total canopy volume, mean and standard deviation of distance between trees, and the number of trees per plot. These were extracted using R software (version 2.15.2) (http://www.r-project.org/).

2.5 Statistical analysis

A modification to the approach outlined in Langton et al. (2010) was used to conduct a 'data mining' exercise to identify important predictor variables for subsequent regression analyses. This was necessary due to the high number of lidar predictor variables and their potential high colinearity with one another, (up to r = 0.9 in many cases). Therefore, the 'MuMin' (Multi-Model Inference) package for R software (version 1.9.5) (http://CRAN.R-project.org/package=MuMIn) was used to run Akaike Information Criterion (AIC) analysis to regress the field data from the 21 plots visited in 2010 against the corresponding lidar metrics. In this case, due to the small number of field plots available, a second order information criterion (AICc) was implemented. AICc incorporates a greater relative penalty for extra parameters, therefore decreasing the probability of selecting models that have too many parameters and might over-fit the data (Burnham & Anderson, 2002). Analyses were performed separately for the DR and FW lidar data. To determine which lidar variables had the most potential for the prediction of forest attributes, an automatic stepwise AICc selection was used on the dataset for 500,000 iterations, where each iteration functioned on a subset of six randomly selected predictor variables. Significant predictors were recorded for each iteration and the variables with the most counts across all iterations identified. For each of the 23 field metrics assessed, a subset of the lidar predictor variables determined to be the most significant (i.e. those with the highest counts) were input into a further stepwise AICc process to derive a final regression equation. Twenty predictor variables determined to be the most significant for each field metric were entered into the stepwise approach. Note that zero values in the field plot data were included in the regression analyses.

The stepwise procedure thus produced a regression model using a subset of the input lidar variables for each field metric. Several criteria were used to examine potential models, including R^2 and adjusted R^2; individual covariate significance (Type III error *t* tests, $p \leq 0.05$); absence of multi-colinearity (i.e. variance inflation factor ≤ 1, see Bowerman & O'Connell, 1990); and residual homoscedasticity. Root Mean Square Error (RMSE) of each model was assessed using the 20 field plots that were not used in establishing the models. The final models selected were those which exhibited a combination of the lowest changes of R^2 to adjusted R^2 and the lowest overall dataset RMSE, whilst still satisfying individual covariate criteria. Adjusted R^2 is considered more conservative than R^2, thus models where the two showed little change were sought when using multiple predictors. The exclusion of redundant covariates was addressed by the examination of individual standard error and variance inflation factor values, as model validity in multiple linear regression relies partly on the number of observations and covariates.

3. Results

Statistical models were developed for each of the 23 field metrics using the DR and FW lidar as separate datasets. Input variables for each model could potentially be drawn from ground, non-ground or all returns, from leaf-on or leaf-off data, for height, intensity/amplitude or echo-width measures, and could also include ITC-derived metrics. A statistically significant model (at $p < 0.05$) was created for all field metrics using the two lidar datasets (DR and FW). Across the 23 field metrics, the R^2 value for the best fit model covered the range $R^2 = 0.43 - 0.94$ for the DR data and $R^2 = 0.28 - 0.97$ for the FW data (Table 3). The normalised RMSE covered the range 18% - 66% for the DR models and 16% - 48% for the FW models. The difference in NRMSE between the best fit DR and FW model was low (≤ 7%) for all but two forest metrics (number of sapling species and number of vascular plant species). It should be noted that for 11 of the 23 forest metrics, the best fit models (i.e. those with the highest R^2) did not generate the best predictions based on independent field validation data, thus demonstrating over-fitting of some models to the input data. This was particularly notable for mean crown horizontal area, standing deadwood decay class, number of sapling species and number of seedling species.

[insert Table 3 here]

Across the 23 best performing models (i.e. those with the lowest NRMSE) the number and composition of input lidar variables differed (Table 4). Thus, all models had between one and four input variables; with 11 models having two input variables, six models having three input variables, and three models each with either one variable (number of tree stems of native species, downed deadwood decay class, and number of vascular plant species) or four variables (number of tree stems, Shannon-Weiner index of diversity, and mean height to the living crown). In terms of the nature of input variables, six of the best performing models had input variables of a single type (i.e. intensity/amplitude, height, echo-width, or ITC-derived), whilst the remaining 17 had input variables of multiple types. In total, 18 of the best performing models contained intensity/amplitude variables, 14 contained height variables, a further 11 contained ITC variables, and 2 contained echo-width variables. Focussing on the timing of lidar input variables; 11 of the best performing models contained only leaf-on data, 10 models contained both leaf-on and leaf-off variables, and 2 models contained only leaf-off data.

[Insert Table 4 here]

Separating the best performing models into those containing DR lidar data (11 models) and those containing FW lidar data (12 models), there was little difference between the two sets of models in the proportional composition of intensity/amplitude, height, echo-width, or ITC-derived input variables (Table 5), and between those point cloud variables derived using all, ground or non-ground lidar returns (Table 6). However, there was a notable difference between the proportion of input variables from leaf-on and leaf-off data between the best performing DR and FW lidar models. Thus, 22 of 26 input variables in the best performing DR models were leaf-on, compared with 18 of 29 input variables in the best performing FW models. In terms of the type of forest metric, 6 of 9 structure metrics were best modelled in DR data, whilst 6 of 10 composition and 3 of 4 deadwood metrics were best modelled in FW data. There was an even division between the two lidar datasets in relation to generating the best performing models across the vegetation layers; thus DR lidar data were used in 6 of 13 canopy layer models, 2 of 3 shrub layer models, and 3 of 7 ground layer models.

[Insert Tables 5 & 6 here]

4. Discussion

As outlined in Matthews & Mackie (2006) there is a requirement for knowledge within a defined area of how many trees exist, what species they are and their relative sizes, in order to make predictions for management purposes. Both structural and compositional information from remote sensing sources have been used in a number of studies to estimate forest inventory metrics, and assess habitat and species presence (Lesak et al., 2011; Martinuzzi et al., 2009). This study has demonstrated the ability of both DR and FW lidar data to estimate multiple forest metrics across a study area.

For the 23 forest metrics investigated here, one was determined with high accuracy (i.e. NRMSE < 20%), 17 with moderate accuracy (NRMSE 20% - 35%), and two with low accuracy (NRMSE > 35%) in the best performing models. Some of this error may have been the result of a 2 year time lag between the collection of both the airborne lidar data and the field plot data used to establish the models (2010) and the field plot data used to validate these models (2012). Also, for many forest variables, the range of data from the field plots surveyed in 2012 was outside that from the field plots surveyed in 2010, which would also have had a likely impact on the estimated prediction accuracy of models established using the 2010 data.

There is extensive surrounding literature on the estimation of forest structural and compositional metrics using airborne lidar data and an area-based regression approach. However, many only predict a relatively limited number of forest metrics (e.g. Hudak et al., 2009; Hyyppä et al., 2008; Li et al., 2014; Lim et al., 2003; Næsset 2004; Richardson &

Moskal, 2011). Thus, no single study has covered such an extensive range of forest metrics as that presented here, especially relating to all vegetation layers in a forest. For those metrics for which direct comparison can be made with other published studies; e.g. number of tree stems (Lee & Lucas, 2007; Næsset, 2002), mean height to the living crown (Andersen et al., 2005; Muss et al., 2011), DBH and basal area (Næsset, 2002; 2004), and downed deadwood volume (Mücke et al., 2013), the prediction accuracy in the current study is of a similar magnitude. Standing deadwood volume was predicted with the highest NRMSE (16%), with three FW lidar variables contributing to the best performing model: skewness of amplitude in non-ground returns (leaf-off), the 25th percentile of echo-width in all returns (leaf-on) and the standard deviation of ITC centroid spacing (leaf on). Thus, standing deadwood is detectable where the return signal strength is low and skewed in relation to surrounding living biomass, and where there is variation in tree spacing. By contrast, the percentage of bare ground cover and number of sapling species were the least well modelled forest measures (with NMRSE of 42% and 48% respectively). Whilst the input lidar variables for the best performing models for these two forest metrics are readily understandable (relating to low order height percentiles, canopy vertical structure, and variation in either amplitude or crown size), these are nonetheless indicators of below canopy conditions in which saplings and ground flora may exist rather than direct measures of the features themselves. The implication here is that variance in overstorey canopy structure indicates structural and compositional diversity in the lower portions of the forest.

In general, the DR and FW lidar datasets performed similarly in terms of the predictive power of the models generated for each forest metric. In total, 12 of the best performing models included FW lidar data whilst the remaining 11 included DR lidar data. There was a slight bias in these models of the DR data towards forest structure variables and the FW data towards compositional and deadwood variables. Nonetheless, in all but two cases (the number of sapling and vascular plant species), the difference in the NRMSE between the best performing DR and FW model was slight (≤ 7%). A disparity existed between sample densities of DR and FW lidar data in this study resulting from fewer FW pulses being recorded. However, small-footprint full waveform lidar data offer a much higher potential for detecting returns beneath the canopy (Wagner et al., 2006). Thus, with the detection of a greater number of return points through Gaussian fitting for the FW lidar data, which provided information along the vector of the laser pulse penetrating the canopy, the distribution of points and total sampled forest elements were different between the DR and FW lidar data in this study. The DR data had a higher horizontal sampling rate at the canopy surface, whilst the FW data had a higher sampling rate through the canopy vertical profile. It was notable that neither DR nor FW data showed a clear advantage at modelling forest metrics at the canopy, shrub or ground level. Thus the perceived advantages of a higher canopy surface sampling rate in the DR data and a higher vertical sampling rate in the FW data for modelling different elements of a forest were not demonstrated as particularly significant in the results of this study. It should be noted, that the reduced sampling rate of the FW data (compared with the DR data) in this study was specific to the lidar system and PRF used for data acquisition. No attempt was made in this study to thin the DR data to the same horizontal sampling rate as the FW data, as the difference between the horizontal and vertical sampling rate of the two datasets and the effect of this when using the data in area-based modelling of forest inventory was the core comparison being made here. Processing techniques to derive usable metrics from FW lidar data for input into forest modelling are still in development, and may provide more metrics beneficial to future analyses, such as the backscatter cross-section or coefficient for each waveform (Alexander et al., 2010; Wagner et al., 2010).

The majority of the best performing statistical models for field metric estimation (i.e. 18 out of 23) involved the use of lidar intensity/amplitude variables from either DR or FW lidar. Moffiet et al. (2005) and Kim et al. (2009a) indicated that the distribution of lidar intensity values in a forest is related to the presence or absence of foliage and its spatial arrangement within the vertical profile, which is dependent on stem density, canopy openness and species types. Hence deadwood biomass volume in a forest context exhibits different lidar intensity values when compared with living biomass (Kim et al., 2009b). Furthermore, Reitberger et al. (2008) showed that lidar return intensity can be used to distinguish between tree bark and coniferous needles, and that the distribution of intensity values could be indicative of broad species types (e.g. coniferous and deciduous), especially under leaf-off conditions. Lidar intensity from the mid-canopy has been shown to be indicative of species number (Brandtberg et al., 2003), whilst intensity metrics from the higher portion of the canopy (in combination with height data) have been shown to make significant contributions to the prediction of forest biomass (Li et al., 2014). The usage of intensity information from small-footprint DR lidar systems remains a somewhat contested issue, however, due to the proprietary methods that commercial systems use to report return intensity which can change in flight, making it impossible to directly compare two returns (Disney et al., 2010). Nonetheless, Kaasalainen et al. (2009) showed the potential to calibrate DR lidar intensity data using reference targets of known backscatter properties from laboratory testing.

FW lidar echo-width metrics were utilised in just two best performing models; standing deadwood volume, and the number of seedling species. FW return echo-width relates to small height variations of scattering elements within the footprint of the laser beam, and is considered a means of inferring surface roughness (Wagner 2010). Mücke et al. (2013) considered the forest ground-level and fallen stems to have smooth surfaces, whereas other vegetated elements, such as shrub vegetation, were considered to be rougher. It should be noted that echo-width metrics were the predictor variables with the smallest contribution in the regression models in this study, and therefore this additional variable only available in FW data may be considered relatively unimportant for forest inventory purposes.

It was notable that almost as many of the best performing models contained ITC-derived variables (11) as contained point cloud height variables (14). All but one of the field metrics relating to tree structure and density (i.e. number of tree stems, their mean spacing, mean DBH, basal area, HTLC, and mean crown horizontal area) utilised plot-level ITC-derived variables within the predictive model equation. Of these, variables related to the horizontal areas of ITC delineated crowns and the spacing between ITC objects were most used in the modelling of tree structural properties. A number of other studies have reported the benefits of using ITC estimates of crown area in addition to variables related to the distribution of height values in the prediction of forest structural characteristics, such as mean DBH and basal area (e.g. Hyyppä et al., 2001; Maltamo et al., 2004). It should be noted that image-based ITC delineation methods, such as those used in this study, have a number of challenges relating to how well both the vertical and horizontal components of a forest can be quantified (Kaartinen et al., 2012), which can constitute a source of error as non-dominant trees are often obscured or incorrectly identified in structurally complex forests.

Almost half of the best performing models (i.e. 10 of 23) utilised a combination of variables produced from both leaf-on and leaf-off datasets. These datasets will capture different properties of the forest when acquired at peak and lowest leaf area, due to the different penetration of the laser pulses through the canopy for both coniferous and deciduous species (where deciduous leaf-loss is typically more obvious) (Næsset, 2005). Lidar data flown under leaf-off conditions are optimal for surface feature mapping, as features close to the ground are less likely to be obscured; likewise this has applications for understorey mapping when data acquisition is appropriately timed (Hill & Broughton, 2009). Kim et al. (2009a) reported that a combination of both leaf-on and leaf-off intensity values gives additional explanatory power when combined in a single model for species differentiation, which goes some way to capturing the variability in multiple forest structural types.

Only relatively basic lidar metrics were used within the context of this study, of which many have also been used within the surrounding literature. There exists a number of alternative methods which could be implemented in future research, such as the detection of vertical layers by examining the return frequencies at different binned heights (or voxels) above ground (e.g. Popescu & Zhao 2008; Wang et al., 2008). In addition, the computation of indices relating to the overall vertical density of vegetative features, e.g. the vertical distribution ratio or height-scaled crown openness index (Lee & Lucas, 2007) may improve model estimates. More complex analysis of the FW waveform could also be performed to derive variables relating to the waveform shape, such as height of median energy, waveform distance, and front slope angle, as used in Cao et al. (2014). There are also a number of alternative approaches available for the estimation of plot-level field metrics, for example the random forest algorithm (Breiman, 2001), whilst more fieldwork samples from the same year as lidar data acquisition would potentially improve the precision and validity of model estimates (Strunk et al., 2012).

5. Conclusions

The approaches used in the current study demonstrate that it is possible to estimate a range of structural, compositional and deadwood forest metrics from airborne lidar data throughout the vertical profile and across a landscape. For 23 metrics examined, statistically significant predictive models were generated for each using both DR and FW lidar datasets in an area-based approach. There was an even division between the best performing models that incorporated DR and FW data, and in all but two cases the difference between the NRMSE of the best performing DR and FW models was slight (i.e. ≤ 7%). The prediction accuracy for the best performing models ranged from an NRMSE of 16% for standing deadwood volume to 48% for the number of sapling species.

Lidar intensity or amplitude variables (DR or FW respectively) were the most numerous selected in the best performing models. However, only two of the best performing models contained the extra intensity-related variable (echo-width) available only from FW lidar data. Although these intensity variables were not calibrated in this study, they were indicative of the presence and distribution of foliar and woody features within the vertical profile. ITC-derived variables were of almost equal importance as plot-level height variables derived from the point cloud in contributing to the best performing models.

Perhaps of greater significance to the choice between lidar data type (i.e. DR or FW) in determining the predictive power of the best performing models was the selection of both leaf-on and leaf-off data. Thus, of the 23 best performing area-based regression models, 10 contained both leaf-on and leaf-off data, whilst 11 contained only leaf-on data. We can therefore conclude that the complimentary information about the entire forest canopy profile that is available from both leaf-on and leaf-off data is of greater benefit to forest inventory in general than the selection between DR or FW lidar data (if used as point clouds). However, this can be forest metric specific.

The area-based method of developing models for the characterisation of forest composition and structure of the selected New Forest field site has direct applications in forest management and for wider objectives (such as forestry and habitat modelling) in other forested regions. Although the models which incorporate lidar intensity are inherently non-transferable because of the lack of calibration, the approach is transferable and could be applied in many environmental contexts and to estimate other forest attributes (e.g. above-ground biomass) or combined into estimates of forest condition.

6. Acknowledgements

We would like to acknowledge the Airborne Research and Survey Facility of the National Environment Research Council for providing the airborne remote sensing datasets, in addition to the assistance of the Forestry Commission for providing site access and supplementary site and management information. We also thank the anonymous reviewers for helpful input into the structuring and content of this manuscript.

7. References

Alexander, C., Tansey, K., Kaduk, J., Holland, D., & Tate, N.J., 2010. Backscatter coefficient as an attribute for the classification of full-waveform airborne laser scanning data in urban areas. *ISPRS Journal of Photogrammetry and Remote Sensing, 64,* 423-432.

Allouis, T., Durrieu, S., Vega, C., & Couteron, P., 2013. Stem volume and above-ground biomass estimation of individual pine trees from LiDAR data: contribution of full-waveform signals. *IEEE Journal of Selected Topics in Applied Earth Observations and Remote Sensing*, *6*, 924-934.

Andersen, H.E., Mcgaughey, R.J., & Reutebuch, S.E., 2005. Estimating forest canopy fuel parameters using lidar data. *Remote Sensing of Environment, 94*, 441-449.

Anderson, J.E., Plourde, L.C., Martin, M.E., Braswell, B.H., Smith, M.L., Dubayah, R.O., Hofton, M.A., & Blair, J.B., 2008. Integrating waveform lidar with hyperspectral imagery for inventory of a northern temperate forest. *Remote Sensing of Environment, 112,* 1856-1870.

Aplin, P., 2005. Remote sensing: ecology. *Progress in Physical Geography, 29,* 104-113.

Armston, J., Disney, M., Lewis, P., Scarth, P., Phinn, S., Lucas, R., Bunting, P., & Goodwin, N. 2013. Direct retrieval of canopy gap probability using airborne waveform lidar. *Remote Sensing of Environment, 134,* 24-38.

Bollandsåsa, O. M., Hanssen K. H., Marthiniussen, S., & Næsset, E., 2008. Measures of spatial forest structure derived from airborne laser data are associated with natural regeneration patterns in an uneven-aged spruce forest. *Forest Ecology and Management. 255,* 953–961.

Bouvier, M., Durrieu, S., Fournier, R.A., & Renaud, J.P., 2015. Generalizing predictive models of forest inventory attributes using an area-based approach with airborne LiDAR data. *Remote Sensing of Environment, 156,* 322-334.

Bowerman, B.L. & O'Connell, R.T., 1990. *Linear Statistical Models: An Applied Approach* (2nd ed.). Belmont, CA: Duxbury.

Brandtberg, T., Warner, T. A., Landenberger, R. E., & Mcgraw, J. B., 2003. Detection and analysis of individual leaf-off tree crowns in small footprint, high sampling density lidar data from the eastern deciduous forest in North America. *Remote Sensing of Environment, 85,* 290-303.

Breiman, L., 2001. Random forests. *Machine Learning, 45,* 5-32.

Bunting, P., Armston, J., Lucas, R.M., & Clewley, D. 2013a. Sorted pulse data (SPD) library. Part I: a generic file format for LiDAR data from pulsed laser systems in terrestrial environments. *Computers and Geosciences, 56,* 197-206.

Bunting, P., Armston, J., Clewley, D., & Lucas, R., 2013b. Sorted pulse data (SPD) library Part II: a processing framework for LiDAR data from pulsed laser systems in terrestrial environments. *Computers and Geosciences, 56,* 207-215.

Burnham, K. P., & Anderson, D. R., 2002. *Model Selection and Multimodel Inference: A Practical Information-Theoretic Approach* (2nd ed.). New York: Springer-Verlag.

Cantarello, E., & Newton, A. C., 2008. Identifying cost-effective indicators to assess the conservation status of forested habitats in Natura 2000 sites. *Forest Ecology and Management, 256,* 815-826.

Cao, L., Coops, N.C., Hermosilla, T., Innes, J., Dai, J., & She, G. 2014. Using small-footprint discrete and full-waveform airborne lidar metrics to estimate total biomass and biomass components in subtropical forests. *Remote Sensing, 6,* 7110-7135.

Chauve, A., Vega, C., Durrieu, S., Bretar, F., Allouis, T., Deseillgny, M.P., & Puech, W., 2009. Advanced full-waveform lidar data echo detection: assessing quality of derived terrain and tree height models in an alpine coniferous forest. *International Journal or Remote Sensing*, *30*, 5211-5228.

Chen, Q., Baldocchi, D., Gong, P., & Kelly, M., 2006. Isolating individual trees in a savanna woodland using small footprint lidar data. *Photogrammetric Engineering and Remote Sensing, 72,* 923-932.

Coops, N., Hilker, T., Wulder, M., St-Onge, B., Newnham, G., Siggins, A., & Troftmow, J., 2007. Estimating canopy structure of Douglas-fir forest stands from discrete-return LiDAR. *Trees 21*, 295–310.

Disney, M. I., Kalogirou, V., Lewis, P., Prieto-Blanco, A., Hancock, S. & Pfeifer, M., 2010. Simulating the impact of discrete-return lidar system and survey characteristics over young conifer and broadleaf forests. *Remote Sensing of Environment*, *114*, 1546-1560.

Estornell, J., Ruiz, L.A., Velazquez-Marti, B., & Fernandez-Sarria, A., 2011. Estimation of shrub biomass by airborne lidar data in small forest stands. *Forest Ecology and Management, 262,* 1697-1703.

Evans, J.S., Hudak, A.T., Faux, R., & Smith, A.M.S., 2009. Discrete return lidar in natural resources: Recommendations for project planning, data processing, and deliverables. *Remote Sensing, 1,* 776-794.

Falkowski, M.J., Evans, J.S., Martinuzzi, S., Gessler, P.E., & Hudak, A.T., 2009. Characterizing forest succession with lidar data: an evaluation for the inland northwest, USA. *Remote Sensing of Environment, 113.* 946-956.

Ferris, R., & Humphrey, J.W., 1999. A review of potential biodiversity indicators for application in British forests. *Forestry, 72,* 313-328.

Ferris, R., Peace, A.J., Humphrey, J.W., & Broome, A., 2000. Relationships between vegetation, site type and stand structure in coniferous plantations in Britain. *Forest Ecology and Management, 136,* 35-51.

Hill, R.A., & Broughton, R.K., 2009. Mapping the understorey of deciduous woodland from leaf-on and leaf-off airborne lidar data: a case study in lowland Britain. *ISPRS Journal of Photogrammetry and Remote Sensing, 64,* 223-233.

Hinsley, S.A., Hill, R.A., Fuller, R.J., Bellamy, P.E., & Rothery, P., 2009. Bird species distributions across woodland canopy structure gradients. *Community Ecology,10,* 99-110.

Hudak, A.T., Crookston, N.L., Evans, J.S., Hall, D.E., & Falkowski, M.J., 2008. Nearest neighbor imputation of species-level, plot-scale forest structure attributes from lidar data. *Remote Sensing of Environment, 112,* 2232-2245.

Hudak, A.T., Evans, J.S., & Smith, A.M.S., 2009. Lidar utility for natural resource managers. *Remote Sensing, 1,* 934-951.

Hyyppä, J., Hyyppä, H., Leckie, D., Gougeon, F., Yu, X., & Maltamo, M., 2008. Review of methods of small-footprint airborne laser scanning for extracting forest inventory data in boreal forests. *International Journal of Remote Sensing, 29,* 1339-1366.

Hyyppä, J., Kelle, O., Lehikoinen, M., & Inkinen, M., 2001. A segmentation-based method to retrieve stem volume estimates from 3-D tree height models produced by laser scanners. *IEEE Transactions on Geoscience and Remote Sensing, 39,* 969-975.

Kaartinen, H., Hyyppä, J., Yu, X.W., Vastaranta, M., Hyyppä, H., Kukko, A., Holopainen, M., Heipke, C., Hirschmugl, M., Morsdorf, F., Næsset, E., Pitkanen, J., Popescu, S., Solberg, S., Wolf, B.M., & Wu, J. C., 2012. An international comparison of individual tree detection and extraction using airborne laser scanning. *Remote Sensing, 4,* 950-974.

Kaasalainen, S., Hyyppä, H., Kukko, A., Litkey, P., Ahokas, E., Hyyppä, J., Lehner, H., Jaakkola, A., Suomalainen, J., Akujarvi, A., Kaasalainen, M., and Pyysalo, U., 2009. Radiometric calibration of lidar intensity with commercially available reference targets. *IEEE Transactions on Geoscience and Remote Sensing, 47,* 588-598.

Kim, S., Mcgaughey, R.J., Andersen, H.E., & Schreuder, G., 2009a. Tree species differentiation using intensity data derived from leaf-on and leaf-off airborne laser scanner data. *Remote Sensing of Environment, 113,* 1575-1586.

Kim, Y., Yang, Z.Q., Cohen, W.B., Pflugmacher, D., Lauver, C.L., & Vankat, J.L., 2009b. Distinguishing between live and dead standing tree biomass on the north rim of Grand Canyon National Park, USA using small-footprint lidar data. *Remote Sensing of Environment, 113,* 2499-2510.

Langton, S.D., Briggs, P.A., & Haysom, K.A., 2010. Daubenton's bat distribution along rivers - developing and testing a predictive model. *Aquatic Conservation-Marine and Freshwater Ecosystems, 20,* 45-54.

Lee, A.C., & Lucas, R.M., 2007. A lidar-derived canopy density model for tree stem and crown mapping in Australian forests. *Remote Sensing of Environment, 111,* 493-518.

Lesak, A.A., Radeloff, V.C., Hawbaker, T.J., Pidgeon, A.M., Gobakken, T., and Contrucci, K., 2011. Modeling forest songbird species richness using lidar-derived measures of forest structure. *Remote Sensing of Environment, 115,* 2823-2835.

Leutner, B.F., Reineking, B., Mueller, J., Bachmann, M., Beierkuhnlein, C., Dech, S. & Wegmann, M. 2012. Modelling forest alpha-diversity and floristic composition - on the added value of lidar plus hyperspectral remote sensing. *Remote Sensing, 4,* 2818-2845.

Li, M., Im, J., Quackenbush, L.J., & Liu, T., 2014. Forest biomass and carbon stock quantification using airborne LiDAR data: a case study over Huntington Wildlife Forest in the Adirondack Park. *IEEE Journal of Selected Tropics in Applied Earth Observations and Remote Sensing. 7,* 3143-3156.

Lim, K., Treitz, P., Baldwin, K., Morrison, I., & Green, J., 2003. Lidar remote sensing of biophysical properties of tolerant northern hardwood forests. *Canadian Journal of Remote Sensing, 29,* 658-678.

Lindberg, E., Olofsson, K., Holmgren, J., & Olsson, H., 2012. Estimation of 3D vegetation structure from waveform and discrete return airborne laser scanning data. *Remote Sensing of Environment, 118,* 151-161.

Matthews, R., & Mackie, E., 2006. *Forest Mensuration: A Handbook for Practitioners*. Edinburgh: HMSO.

Mallet, C., Lafarge, F., Roux, M., Soergel, U., Bretar, F., & Heipke, C., 2010. A marked point process for modelling lidar waveforms. *IEEE Transactions on Image Processing, 19,* 3204-3221.

Maltamo, M., Eerikainen, K., Pitkanen, J., Hyyppä, J., & Vehmas, M., 2004. Estimation of timber volume and stem density based on scanning laser altimetry and expected tree size distribution functions. *Remote Sensing of Environment, 90,* 319-330.

Maltamo, M., Packalen, P., Yu, X., Eerikainen, K., Hyyppä, J., & Pitkanen, J., 2005. Identifying and quantifying structural characteristics of heterogeneous boreal forests using laser scanner data. *Forest Ecology and Management, 216,* 41-50.

Martinuzzi, S., Vierling, L.A., Gould, W.A., Falkowski, M.J., Evans, J.S., Hudak, A.T., & Vierling, K. T., 2009. Mapping snags and understory shrubs for a lidar-based assessment of wildlife habitat suitability. *Remote Sensing of Environment, 113,* 2533-2546.

Miura, N., & Jones, S.D., 2010. Characterizing forest ecological structure using pulse types and heights of airborne laser scanning. *Remote Sensing of Environment, 114,* 1069-1076.

Moffiet, T., Mengersen, K., Witte, C., King, R., & Denham, R., 2005. Airborne laser scanning: Exploratory data analysis indicates potential variables for classification of individual trees or forest stands according to species. *ISPRS Journal of Photogrammetry and Remote Sensing, 59,* 289-309.

Mücke, W., Deak, B., Schroiff, A., Hollaus, M. & Pfeifer, N. 2013. Detection of fallen trees in forested areas using small footprint airborne laser scanning data. *Canadian Journal of Remote Sensing, 39,* 32-40.

Muss, J. D., Mladenoff, D.J., & Townsend, P. A., 2011. A pseudo-waveform techniques to assess forest structure using discrete lidar data. *Remote Sensing of Environment. 115,* 824-835.

Næsset, E., 2002. Predicting forest stand characteristics with airborne scanning laser using a practical two-stage procedure and field data. *Remote Sensing of Environment, 80,* 88-99.

Næsset, E., 2004. Practical large-scale forest stand inventory using a small-footprint airborne scanning laser. *Scandinavian Journal of Forest Research, 19,* 164-179.

Næsset, E., 2005. Assessing sensor effects and effects of leaf-off and leaf-on canopy conditions on biophysical stand properties derived from small-footprint airborne laser data. *Remote Sensing of Environment, 98*, 356-370.

Næsset, E., 2007. Airborne laser scanning as a method in operational forest inventory: Status of accuracy assessments accomplished in Scandinavia. *Scandinavian Journal of Forest Research*, *22*, 433-442.

Næsset, E., 2009. Effects of different sensors, flying altitudes, and pulse repetition frequencies on forest canopy metrics and biophysical stand properties derived from small-footprint airborne laser data. *Remote Sensing of Environment*, *113*, 148-159.

Newton, A.C., Cantarello, E., Myers, G., Douglas, S., & Tejedor, N., 2010. The condition and dynamics of new forest woodlands. In: Newton, A. C. ed. *Biodiversity in the New Forest.* Newbury, Berkshire: Pisces Publications, pp. 132-147.

Newton, A.C., Hill, R.A., Echeverria, C., Golicher, D., Benayas, J.M.R., Cayuela, L., & Hinsley, S.A., 2009. Remote sensing and the future of landscape ecology. *Progress in Physical Geography*, *33*, 528-546.

Persson, Å., Holmgren, J., & Soderman, U., 2002. Detecting and measuring individual trees using an airborne laser scanner. *Photogrammetric Engineering and Remote Sensing, 68,* 925-932.

Pesonen, Å., Maltamo, M., Eerikainen, K., & Packalen, P., 2008. Airborne laser scanning-based prediction of coarse woody debris volumes in a conservation area. *Forest Ecology and Management, 255,* 3288-3296.

Popescu, S.C., & Zhao, K., 2008. A voxel-based lidar method for estimating crown base height for deciduous and pine trees. *Remote Sensing of Environment, 112*, 767-781.

Popescu, S.C., Wynne, R.H., & Scrivani, J.A., 2004. Fusion of small-footprint lidar and multispectral data to estimate plot-level volume and biomass in deciduous and pine forests in Virginia, USA. *Forest Science, 50*, 551–565

Reitberger, J., Krzystek, P., & Stilla, U., 2008. Analysis of full waveform lidar data for the classification of deciduous and coniferous trees. *International Journal of Remote Sensing, 29*, 1407-1431.

Richardson, J.J., & Moskal, L.M., 2011. Strengths and limitations of assessing forest density and spatial configuration with aerial lidar. *Remote Sensing of Environment, 115,* 2640-2651.

Shannon, C.E., 1948. The mathematical theory of communication. In: Shannon, C. E., and Weaver, W. eds. *The Mathematical Theory of Communication.* Urbana: University of Illinois Press, *pp. 29-125.*

Simpson, E. H., 1949. Measurement of diversity. *Nature*, *163*, 688.

Spies, T., Franklin, J. & Thomas, T., 1988. Coarse woody debris in Douglas-fir forests of western Oregon and Washington. *Ecology, 69,* 1689-1702.

Strunk, J., Temesgen, H., Andersen, H.E., Flewelling, J.P., & Madsen, L., 2012. Effects of lidar pulse density and sample size on a model-assisted approach to estimate forest inventory variables. *Canadian Journal of Remote Sensing, 38,* 644-654.

Tubbs, C. R., 2001. *The New Forest. History, Ecology, and Conservation.* Lyndhurst, Hampshire: New Forest Ninth Centenary Trust.

Wagner, W., 2010. Radiometric calibration of small-footprint full-waveform airborne laser scanner measurements. *ISPRS Journal of Photogrammetry and Remote Sensing, 65,* 505-513.

Wagner, W., Hollaus, M., Briese, C., & Ducic, V., 2008. 3D vegetation mapping using small-footprint full-waveform airborne laser scanners. *International Journal of Remote Sensing*, *29*, 1433-1452.

Wagner, W., Ullrich, A., Ducic, V., Melzer, T., & Studnicka, N., 2006. Gaussian decomposition and calibration of a novel small-footprint full-waveform digitising airborne laser scanner. *ISPRS Journal of Photogrammetry and Remote Sensing*, *60*, 100-112.

Wang, Y.S., Weinacker, H., & Koch, B., 2008. A lidar point cloud based procedure for vertical canopy structure analysis and 3d single tree modelling in forest. *Sensors*, *8*, 3938-3951.

Yu, X., Litkey, P., Hyyppä, J., Holopainen, M., & Vastaranta, M., 2014. Assessment of low density full-waveform airborne laser scanning for individual tree detection and tree species classification. *Forests*, *5*, 1011-1031.

Zhang, K. Q., Chen, S. C., Whitman, D., Shyu, M. L., Yan, J. H., & Zhang, C. C., 2003. A progressive morphological filter for removing non-ground measurements from airborne lidar data. *IEEE Transactions on Geoscience and Remote Sensing*, *41*, 872-882.

Tables

Table 1. Summary of field data enumerated across the 21 plots surveyed in 2010 (used to establish regression-based relationships with airborne lidar data) and the 20 plots surveyed in 2012 (used to validate the regression-based relationships with airborne lidar data).

Field metric name	Forest layer	Metric type	2010 field plots				2012 field plots			
			Min	Max	Mean	St. Dev.	Min	Max	Mean	St. Dev.
Number of tree stems	Canopy	Structure	7	52	24.86	11.12	16	90	32.20	18.86
Mean tree stem spacing (m)	Canopy	Structure	2.65	8.45	4.09	1.33	1.84	5.17	3.20	1.05
Number of tree species	Canopy	Composition	1	7	3.52	1.40	1	5	3.45	1.28
Number of tree stems of native species	Canopy	Composition	2	34	15.67	9.46	0	52	19.85	12.66
Shannon-Wiener index of diversity	Canopy	Composition	0.00	1.47	0.86	0.39	0.00	1.43	0.86	0.41
Simpson index of diversity	Canopy	Composition	0.00	1.00	0.50	0.27	0.00	1.29	0.73	0.36
Mean height to the living crown (m)	Canopy	Structure	3.30	13.94	8.00	3.20	2.83	13.46	7.78	3.10
Mean crown horizontal area (m^2)	Canopy	Structure	23.61	119.91	57.52	28.96	13.03	100.11	49.67	23.55
Total crown horizontal area (m^2)	Canopy	Structure	590.17	2198.75	1219.05	402.72	658.59	2102.26	2136.94	382.30
Mean DBH (cm)	Canopy	Structure	27.45	61.84	40.06	9.41	18.72	47.86	33.71	29.14
Plot level basal area (m^2)	Canopy	Structure	2.10	5.24	3.28	0.83	2.06	5.27	3.26	0.86
Standing deadwood volume (m^3)	Canopy	Deadwood	0.00	10.12	1.93	3.22	0.00	8.27	0.87	1.97
Standing deadwood decay class (1-3)	Canopy	Deadwood	0.00	2.88	2.19	0.42	0.00	3.00	0.74	0.18
Downed deadwood volume (m^3)	Ground	Deadwood	0.09	14.62	3.54	4.58	0.22	38.42	4.44	8.29
Downed Deadwood decay class (1-3)	Ground	Deadwood	1.56	2.85	2.34	0.39	0.48	2.85	0.68	0.11
Number of sapling stems	Shrub	Structure	0	42	4.33	9.31	0	108	9.85	24.74
Number of sapling species	Shrub	Composition	0	4	1.00	1.22	0	3	1.00	0.97
Number of sapling stems of native species	Shrub	Composition	0	34	3.86	7.72	0	38	2.90	8.45
Number of seedling stems	Ground	Structure	9	864	145.29	206.44	0	936	339.70	297.62
Number of seedling species	Ground	Composition	1	7	2.05	1.40	0	13	4.40	2.89
Number of seedling stems of native species	Ground	Composition	9	405	109.29	123.94	0	936	230.60	278.95
Number of vascular plant species	Ground	Composition	2	6	3.86	1.35	2	8	4.56	1.82
Percentage bare ground cover (%)	Ground	Composition	0	90	21.69	26.45	0	95	43.50	38.01

Table 2. Summary of the sampling rate for DR and FW lidar data under leaf-on and leaf-off conditions, and the number of returns generated from the resulting point clouds. These values include data for overlapping flight-lines and are average values across the entire field site (i.e. including forest and non-forest areas).

Lidar data	**Leaf-on**			**Leaf-off**		
	No. of pulses per m^2	**No. of derived points per m^2**	**1st returns as a % of the point cloud**	**No. of pulses per m^2**	**No. of derived points per m^2**	**1st returns as a % of the point cloud**
DR	4.97	6.02	82.5%	5.25	7.57	69.4%
FW	2.43	5.09	47.7%	2.51	6.50	38.6%

Table 3. Summary of R^2, RMSE and NRMSE for the best performing regression model produced from the DR and FW lidar data. All models shown are significant at $p < 0.05$. The values underlined show the best performing model per field metric.

	DR lidar			***FW lidar***		
Field metric	$\mathbf{R^2}$	**RMSE**	**NRMSE**	$\mathbf{R^2}$	**RMSE**	**NRMSE**
Number of tree stems	0.67	18.04	24%	0.67	15.97	22%
Mean tree stem spacing (m)	0.91	1.71	40%	0.91	1.32	33%
Number of tree species	0.43	1.50	25%	0.32	1.66	28%
Number of tree stems of native species	0.55	15.05	29%	0.61	13.93	27%
Shannon-Wiener index of diversity	0.57	0.53	37%	0.67	0.58	40%
Simpson index of diversity	0.59	0.31	24%	0.55	0.29	22%
Mean height to the living crown (m)	0.88	2.68	25%	0.88	2.54	24%
Mean crown horizontal area (m^2)	0.63	23.53	27%	0.86	24.39	28%
Total crown horizontal area (m^2)	0.75	561.55	39%	0.69	645.64	45%
Mean DBH (cm)	0.80	9.71	33%	0.80	10.11	35%
Plot level basal area (m^2)	0.66	0.83	26%	0.69	0.91	28%
Standing deadwood volume (m^3)	0.91	1.50	18%	0.92	1.36	16%
Standing deadwood decay class (1-3)	0.88	0.72	36%	0.59	0.57	29%
Downed deadwood volume (m^3)	0.51	2.74	30%	0.45	2.49	27%
Downed Deadwood decay class (1-3)	0.79	0.51	36%	0.75	0.60	43%
Number of sapling stems	0.92	24.41	23%	0.97	26.46	25%
Number of sapling species	0.94	1.99	66%	0.70	1.42	48%
Number of sapling stems of native species	0.90	10.40	27%	0.97	11.47	30%
Number of seedling stems	0.82	295.24	32%	0.28	331.96	36%
Number of seedling species	0.74	3.16	24%	0.45	3.10	24%
Number of seedling stems of native species	0.63	239.08	33%	0.68	245.15	34%
Number of vascular plant species	0.75	2.36	39%	0.77	1.70	28%
Percentage bare ground cover (%)	0.76	44.04	46%	0.86	39.82	42%

Table 4. The input predictor variables used in the 23 best performing regression models (i.e. those which produced estimates with the smallest RMSE)

Estimated field metric name	**Field metric type**	**Data set used in the model**	**Model input variables**
Number of tree stems	Structure	FW lidar	(1) mean ITC horizontal area (leaf-on); (2) 20th height percentile [all returns] (leaf-on); (3) kurtosis of amplitude [non-ground returns] (leaf-off); (4) skewness of height [non-ground returns] (leaf-off).
Mean tree stem spacing (m)	Structure	FW lidar	(1) mean spacing of ITC centroids (leaf on); (2) 20th amplitude percentile [all returns] (leaf-off).
Number of tree species	Composition	DR lidar	(1) 50th height percentile [all returns] (leaf-off); (2) variance of intensity [non-ground returns] (leaf-on).
Number of tree stems of native species	Composition	FW lidar	(1) kurtosis of height [all returns] (leaf-on).
Shannon-Wiener index of diversity	Composition	DR lidar	(1) median height [non-ground returns] (leaf-off); (2) skewness of intensity [non-ground returns] (leaf-on); (3) total ITC horizontal area (leaf-on); (4) total ITC volume (leaf-on).
Simpson index of diversity	Composition	FW lidar	(1) skewness of amplitude [non-ground returns] (leaf-on); (2) total ITC horizontal area (leaf-on); (3) variance of height [all returns] (leaf-on).
Mean height to the living crown (m)	Structure	FW lidar	(1) maximum vertical gap identified in the vertical height profile (leaf-off); (2) mean spacing of ITC centroids (leaf-on); (3) ITC mean canopy geometric volume (leaf-on), (4) variance of amplitude [non-ground returns] (leaf-on).
Mean crown horizontal area (m^2)	Structure	DR lidar	(1) kurtosis of intensity [non-ground return] (leaf-off); (2) mean spacing of ITC centroids (leaf-on); (3) total ITC horizontal area (leaf-on).
Total crown horizontal area (m^2)	Structure	DR lidar	(1) mean height [all returns] (leaf-on); (2) standard deviation of height [all returns] (leaf-on); (3) variance of intensity [all returns] (leaf-on).

Mean DBH (cm)	Structure	DR lidar	(1) mean spacing of the ITC centroids (leaf-on); (2) ITC mean canopy geometric volume (leaf-on).
Plot level basal area (m^2)	Structure	DR lidar	(1) 55th intensity percentile [all returns] (leaf-on); (2) mean spacing of ITC centroids (leaf-on).
Standing deadwood volume (m^3)	Deadwood	FW lidar	(1) skewness of amplitude [non-ground returns] (leaf-off); (2) standard deviation of the ITC centroids spacing (leaf-on); (3) 25th percentile echo-width [all returns] (leaf-on).
Standing deadwood decay class (1-3)	Deadwood	FW lidar	(1) 35th amplitude percentile [all returns] (leaf-on); (2) 20th height percentile [all returns] (leaf-on).
Downed deadwood volume (m^3)	Deadwood	FW lidar	(1) skewness of amplitude [non-ground return] (leaf-off); (2) absolute deviation of heights [all returns] (leaf-off).
Downed Deadwood decay class (1-3)	Deadwood	DR lidar	(1) mean intensity [non-ground returns] (leaf-on).
Number of sapling stems	Structure	DR lidar	(1) 60^{th} percentile for intensity [all returns] (leaf-on), (2) 60^{th}height percentile [all returns] (leaf-on), (3) mean intensity [all returns] (leaf-on).
Number of sapling species	Composition	FW lidar	(1) 35^{th} height percentile [all returns] (leaf-on); (2) variance of amplitude [all returns] (leaf-off).
Number of sapling stems of native species	Composition	DR lidar	(1) 60^{th} intensity percentile [all returns] (leaf-on); (2) median height [non-ground returns] (leaf-on);
Number of seedling stems	Structure	DR lidar	(1) mean absolute deviation of intensity [ground returns] (leaf-off); (2) mean of intensity [ground returns] (leaf-on).
Number of seedling species	Composition	FW lidar	(1) mean amplitude [ground returns] (leaf-off); (2) standard deviation of echo-width [ground returns] (leaf-off).
Number of seedling stems of native species	Composition	DR lidar	(1) standard deviation of ITC spacing (leaf-on); (2) mean ITC canopy geometric volume (leaf-on).
Number of vascular plant species	Composition	FW lidar	(1) variance of heights [non-ground returns] (leaf-on)
Percentage bare ground cover (%)	Composition	FW lidar	(1) 20^{th} height percentile [all returns] (leaf-on); (2) height of largest vertical gap in return height profile (leaf-off); (3) standard deviation of ITC area (leaf-on conditions).

Table 5. The number of input variables used in the 23 best performing models by variable category. Percentage contribution is shown in parentheses.

Data set used in the model	ITC variables (from raster)	Height variables (from point cloud)	Intensity/amplitude variables (from point cloud)	Echo-width variables (from point cloud)	Total
DR	9 (35%)	6 (23%)	11 (42%)	-	26
FW	7 (24%)	11 (38%)	9 (31%)	2 (7%)	29

Table 6. The number of variables using ground, non-ground and all returns used as inputs to the 23 best performing models. Percentage contribution is shown in parentheses.

Data set used in the model	Ground	Non-ground	All	Total
DR	2 (12%)	6 (35%)	9 (53%)	17
FW	2 (9%)	7 (32%)	13 (59%)	22

Figure 1

Sample cross section (100 m x 20 m) of a point cloud from leaf-on DR lidar data (top) and FW lidar data (bottom). Points classified as ground or non-ground are indicated.

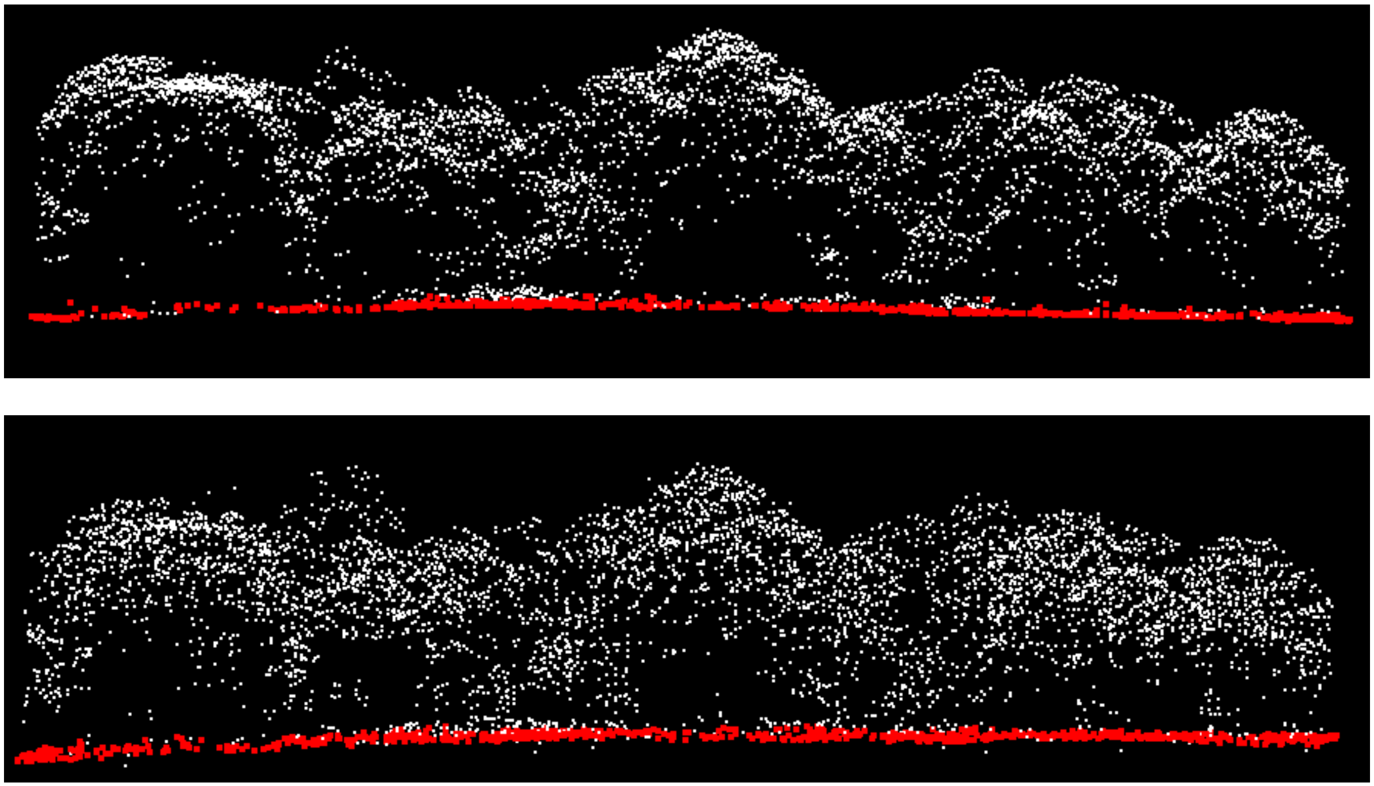

Figure

Click here to download high resolution image